NMR structural elucidation of dehydrodimers resulting from oxidation of 5-O-caffeoylquinic acid in an apple juice model solution

Claudia Mariana Castillo-Fraire, Sandrine Pottier, Arnaud Bondon, Erika Salas, Stéphane Bernillon, Sylvain Guyot, Pascal Poupard

Journal Pre-proofs

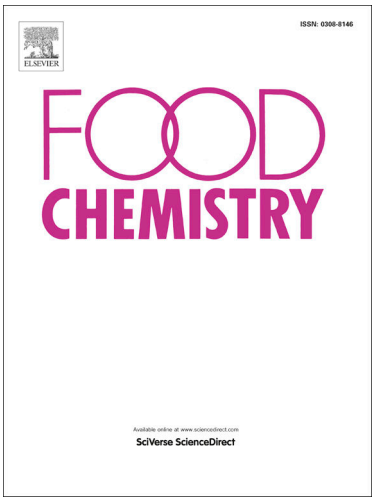

NMR structural elucidation of dehydrodimers resulting from oxidation of 5-*O*-caffeoylquinic acid in an apple juice model solution

Claudia Mariana Castillo-Fraire, Sandrine Pottier, Arnaud Bondon, Erika Salas, Stéphane Bernillon, Sylvain Guyot, Pascal Poupard

PII: S0308-8146(21)02123-3
DOI: https://doi.org/10.1016/j.foodchem.2021.131117
Reference: FOCH 131117

To appear in: *Food Chemistry*

Received Date: 10 March 2021
Revised Date: 13 August 2021
Accepted Date: 8 September 2021

Please cite this article as: Castillo-Fraire, C.M., Pottier, S., Bondon, A., Salas, E., Bernillon, S., Guyot, S., Poupard, P., NMR structural elucidation of dehydrodimers resulting from oxidation of 5-*O*-caffeoylquinic acid in an apple juice model solution, *Food Chemistry* (2021), doi: https://doi.org/10.1016/j.foodchem.2021.131117

NMR structural elucidation of dehydrodimers resulting from oxidation of 5-*O*-caffeoylquinic acid in an apple juice model solution

Claudia Mariana Castillo-Fraire [a,c], Sandrine Pottier [d,e], Arnaud Bondon [d,e], Erika Salas [f], Stéphane Bernillon [g], Sylvain Guyot [a,c,*], Pascal Poupard [b,c]

[a] INRAE UR BIA − Polyphenols, Reactivity, Processes, F-35653, Le Rheu, France

[b] IFPC (French Institute for Cider Production), F-35653, Le Rheu, France

[c] UMT ACTIA Nova²Cidre, F-35653, Le Rheu, France

[d] Univ Rennes 1, COrInt, ISCR UMR CNRS 6226, Rennes, France

[e] Univ Rennes 1, Plateforme PRISM, SFR UMS CNRS 3480, INSERM 018, Biosit, Rennes, France

[f] Facultad de Ciencias Químicas, Universidad Autónoma de Chihuahua, Circuito Universitario s/n, Campus Universitario No. 2, CP 31125, Chihuahua, México

[g] UMR1332 Biologie du Fruit et Pathologie, INRAE, Université de Bordeaux, Centre INRAE de Nouvelle Aquitaine-Bordeaux, Villenave d'Ornon, France

* Corresponding author at INRAE UR1268 BIA − Polyphenols, Reactivity, Processes, F-35653, Le Rheu, France. E-mail address: sylvain.guyot@inrae.fr (S. Guyot)

Keywords: phenolic compounds, CQA dehydrodimers, chlorogenic acid, PPO, caffeicin

ABSTRACT

During apple juice and cider-making processes, phenolic compounds undergo enzymatic oxidation. 5-*O*-caffeoylquinic acid (CQA) is one of the major hydroxycinnamic acid derivatives and it is the preferential substrate for polyphenol oxidase (PPO) in apple juices. Consequently, CQA dehydrodimers (MW 706 Da) are among the main products resulting from CQA oxidation.

CQA dehydrodimers were previously synthesized in a biomimetic apple juice model solution. Following their purification and characterization using UV-Visible spectra and mass spectrometry, the structures of seven CQA dehydrodimers were elucidated using ^{1}H and ^{13}C one- and two-dimensional NMR spectroscopy. Six of them exhibited dihydrobenzofuran, benzodioxane, or dihydronaphtalene skeletons, which are caffeicin-like structures. Interestingly,

a new dehydrodicaffeoylquinic acid molecule was also characterised for which two novel structures showing a symmetric dicatechol skeleton were also proposed.

1 Introduction

Chlorogenic acids (CGA) are a group of phenolic acids that correspond to hydroxycinnamic acids esterified by a quinic acid moiety. These widespread compounds are present in plants, fruits, and vegetables, and are characteristic compounds in coffee beans, tea, maté, blueberries, cherries, plums, pears, apples, spinach, and potato tubers (Clifford, 1999, 2000). CGA are known to have bioactive properties such as antioxidant, free radical-scavenging, antibacterial, and antidiabetic properties, as well as neuroprotective activity (Bao et al., 2018; Naveed et al., 2018). Regarding apple and apple-derived products, the major hydroxycinnamic acid derivative is 5-*O*-caffeoylquinic acid (CQA). Depending on the apple variety, CQA concentrations range from 200 to 1000 mg/L in apple juices (Guyot et al., 2008).

During the first step of apple juice production (crushing, pressing), polyphenols come into contact with polyphenol oxidase (PPO). In this step, CQA, the preferential substrate for PPO, can be oxidised into its corresponding ortho-quinone in presence of oxygen. This highly reactive species can be involved in different reaction pathways leading to the formation of a multiplicity of neoformed molecules (Poupard et al., 2008). However, the detailed structures and properties of these oxidation products are yet little known.

Oxidation products have been explored in synthetic solutions using caffeic acid as a model compound (Cilliers & Singleton, 1991; Fulcrand et al., 1994; Pati et al., 2006; Weber et al., 2019). Some of these oxidised products have been characterised using several techniques: UV-Visible spectra, (Cilliers & Singleton, 1991; Fulcrand et al., 1994; Pati et al., 2006), mass spectrometry (Pati et al., 2006), and NMR (Cilliers & Singleton, 1991; Fulcrand et al., 1994). Their characterization has highlighted that they are mainly dehydrodimers resulting from oxidative coupling whose linkage could involve the aromatic ring and/or the double bond of the propenoic acid chain. Most of them have been classified

as caffeicin and correspond to dihydrobenzofuran, dihydrobenzodioxan, or dihydronaphtalene types (Cilliers & Singleton, 1991).

In apple juice, caffeoylquinic acid oxidation products were first detected using LC/MS analyses (Bernillon et al., 2004). These compounds were then synthesized in an apple juice model solution. LC/MS analyses confirmed the molecular weight of 706 Da, suggesting that these compounds correspond to oxidative coupling between two CQA molecules (Castillo-Fraire et al., 2019; Wong-Paz et al., 2015). Their tanning properties have been explored previously, highlighting a specific interaction with certain families of salivary proteins (Castillo-Fraire et al., 2021).

In our previous research, sufficient quantities of CQA oxidation products were synthesized enzymatically for purification on a milligram scale. Centrifugal Partition Chromatography (CPC) was optimised to fractionate these CQA dehydrodimers (Castillo-Fraire et al., 2019). After preparative/semi-preparative HPLC, ten CQA dehydrodimers with a chromatographic purity higher than 85% were successfully recovered (Castillo-Fraire et al., 2019).

In this work, we present the structure elucidation of seven of these CQA dehydrodimers using Nuclear Magnetic Resonance (NMR).

2 Material and Methods

2.1 Chemicals and enzymes

5-*O*-caffeoylquinic acid (CQA) was obtained from Sigma-Aldrich (St. Louis, MO, USA) and the crude extract of polyphenol oxidase (PPO) was prepared in our laboratory as described previously (Le Bourvellec et al., 2004). HPLC-grade solvents for the purification of the CQA oxidation products (Castillo-Fraire et al., 2019) and methanol for the NMR analyses were purchased from Eurisotop (Saint-Aubin, France).

2.2 Synthesis and purification of CQA oxidation products

The complete procedure has been described in detail in a previous study published recently (Castillo-Fraire et al., 2019). Briefly, CQA dehydrodimers were synthesized by enzymatic oxidation (PPO) of

CQA in a model solution (Figure 1). The remaining CQA was eliminated using Centrifugal Partition Chromatography (CPC) performed in Elution-Extrusion Counter Current Chromatography (EECCC) mode. Finally, purification was sharpened using preparative/semi-preparative HPLC.

The ten CQA dehydrodimers were eluted between 14 min and 46 min (10–33 % ACN), suggesting a wide dispersion of polarity. The polarity of most of the compounds was lower than their precursors, except for 705-1 and 705-1.1 that were eluted before CQA in the LC/MS analysis. The compound number indicates the order of elution.

2.3 NMR analyses

To elucidate their structures, seven CQA dehydrodimers (705-1, 705-1.1, 705-2, 705-3, 705-4, 705-5, and 705-6) were analysed using NMR. Samples were dissolved in deuterated methanol (CD_3OD). NMR spectra were recorded at 298 K and measurements were carried out on a Bruker AVANCE 500 spectrometer (Bruker, Wissembourg, France) with a Triple Resonance (TCI) 5 mm cryoprobe (^{1}H, ^{13}C, ^{15}N). The chemical shifts were attributed using 2D Homo-nuclear and Hetero-nuclear spectra: DQF-COSY, TOCSY, edited ^{13}C-HSQC, ^{13}C-HSQC-TOCSY, and ^{13}C-IMPACT-HMBC. Standard pulse sequences from the Bruker database were used. Chemical shifts were expressed as ppm and the spectra were processed using Topspin software.

3 Results and discussion

3.1 NMR analyses

In a previous study based on UV-Visible spectra and MS^n spectrometry, three hypothetical structures were proposed for 9 out of the 10 dehydrodimers purified (Castillo-Fraire et al., 2019). In the present study, NMR spectrometry confirmed these structural hypotheses. In addition, NMR was successfully used to propose two novel structural hypotheses. Table 1 shows ^{1}H proton and ^{13}C carbon chemical shifts for the seven compounds analysed. A dihydronaphtalene-type structure (Figure 4) was proposed for compounds 705-1 and 705-1.1, a dihydrobenzofuran-type structure (Figure 2) for dehydrodimers

705-3 and 705-4, and a dihydrobenzodioxane-type structure (Figure 3) for dehydrodimers 705-5 and 705-6.

As dehydrodimer 705-2 presented a completely different MS^n fragmentation and UV-Visible spectrum compared to the other CQA dehydrodimers, no hypothetical structure was proposed for this compound in our previous study (Castillo-Fraire et al., 2019). NMR spectrometry analyses were necessary to elucidate its structure.

3.1.1 Structure elucidation of the dihydrobenzufuran-type dehydrodimers

These compounds presented UV–vis spectra with a λmax at 327 nm (Castillo-Fraire et al., 2019). The detailed structure of products 705-3 and 705-4 (Figure 2A) was elucidated from the ^1H and ^{13}C NMR spectra. The chemical shifts of the carbon and proton atoms are presented in Table 1. The structural analyses of 705-3 and 705-4 have been discussed in a previous paper (Castillo-Fraire et al., 2019). MS^n fragmentation highlighted that they likely correspond to two CQA dehydrodimer isomers with a dihydrobenzofuran moiety. The MS^n transitions for 705-3 and 705-4 were 705→513→339→295 (Castillo-Fraire et al., 2019). These compounds are analogues of caffeic acid oxidation products (caffeicin F) already described by Cilliers and Singleton (1991).

In the following paragraph, all ^1H and ^{13}C chemical shifts are given for isomer 705-3. The corresponding chemical shifts for isomer 705-4 are listed in Table 1.

The ^{13}C NMR signal at 167.09 ppm was used as a starting point for the structure elucidation. It corresponds to a strongly deshielded carbon consistent with an ester group. Moreover, the HMBC spectrum showed a clear correlation of this carbon (167.09 ppm) with two adjacent protons showing a large coupling constant ^2J (15.9 Hz) consistent with α-β ethylene protons. This carbon (167.09 ppm) was thus identified as C9 (Figure 2A) and the two protons at 7.62 ppm and 6.35 ppm were attributed to H7 and H8. HMBC correlations allowed H8 (6.35 ppm) to be unambiguously distinguished from

H7 (7.62 ppm), as the latter was the only one showing HMBC correlations with 5 carbons (128.45, 116.06, 116.62, 114.78, 167.09 ppm). On the ^{1}H-^{13}C HSQC spectrum, carbons C7 and C8 correlated with H7 and H8 were observed at 145.27 ppm and 114.78 ppm, respectively. The signal at 128.45 ppm was attributed to the quaternary carbon C1 (no correlation on ^{1}H-^{13}C HSQC spectrum).

On the ^{1}H-^{13}C HMBC spectrum, the ^{13}C signals of carbons C2 and C6 were detected at 116.06 ppm and 116.62 ppm, respectively. The distinction between these two carbons was based on the fact that only carbon C6 (116.62 ppm) was correlated to a moderately deshielded proton (4.37 ppm). From the ^{1}H-^{13}C HSQC spectrum, the signals at 7.06 and 7.21 ppm could be attributed to H2 and H6, respectively. Proton H2 (7.06 ppm) was also correlated to ^{13}C signals at 141.64 ppm and 149.36 ppm corresponding to carbons C3 and C4. The ^{13}C signal at 149.36 ppm was attributed to carbon C4 as it is the only carbon showing an expected correlation with H6. Then, the ^{13}C signal at 141.64 ppm was attributed to C3.

Proton H6 (7.21 ppm) on the ^{1}H-^{13}C HMBC spectrum was correlated to a weakly deshielded carbon at 55.65 ppm and the ^{1}H-^{13}C HSQC spectrum revealed that this carbon at 55.65 ppm was linked to the moderately deshielded proton at 4.37 ppm. The latter proton and carbon were thus temporarily attributed to the 8' position. According to the ^{1}H-^{13}C HMBC spectrum, this proton (H8') was correlated to six carbons. The most deshielded one (170.57 ppm) was attributed to C9', which is consistent with an ester group. The latter carbon (C9') was correlated to a ^{1}H signal at 6.05 ppm, which could be temporarily attributed to H7'. Indeed, this proton (H7') was also correlated to six other carbons (55.65, 112.58, 117.34, 126.20, 131.78, and 149.36 ppm) (Figure 2B). Among them, three corresponded to quaternary carbons (126.20, 131.78, and 149.36 ppm). Only one carbon (131.78 ppm) was correlated to three aromatic protons (6.79, 6.79, and 6.86 ppm) allowing its identification as C1'. The signals of the three aromatic protons were consistent with a catechol group. Proton H2' was unambiguously identified at 6.86 ppm and a doublet with a small ^{3}J coupling constant (1.5 Hz) was observed. Even if the signals of protons H6' and H5' overlapped at 6.79 ppm, they were assigned

based on their coupling constants. H6' presented two coupling constants (8.1 Hz and 1.5 Hz) and H5 only one (8.1 Hz). In addition, the whole signal integration of this zone (from 6.76 to 6.80 ppm) was consistent with the signal of two protons. The corresponding carbons C2', C5', and C6' were attributed to chemical shifts at 112.58, 114.97, and 117.34 ppm, respectively, according to the ^{1}H-^{13}C HSQC spectrum. The attribution of proton H7' was confirmed thanks to its correlation with both C2' and C6' unambiguously observed on the ^{1}H-^{13}C HMBC spectrum. Consequently, the attribution of proton H8' was also confirmed. Indeed, this proton (H8') was correlated to two carbons already identified (C6 at 116.62 ppm and C4 at149.36 ppm) and four other carbons (86.96, 126.20, 131.78, and 170.57 ppm) according to the ^{1}H-^{13}C HMBC spectrum.

3.1.2 Structure elucidation of the dihydrobenzodioxane-type dehydrodimers

These compounds presented UV–vis spectra with λmax close to 291 nm and 317 nm (Castillo-Fraire et al., 2019). These spectra are similar to those of the four caffeicin (A–D) identified by Cilliers and Singleton (1991). The detailed structures of products 705-5 and 705-6 (Figure 3A) were elucidated from the ^{1}H and ^{13}C NMR spectra. The chemical shifts of the ^{13}C and ^{1}H atoms are presented in Table 1. The structural analyses of 705-5 and 705-6 have been discussed in a previous paper (Castillo-Fraire et al., 2019). MS^{n} fragmentation revealed that they likely correspond to two CQA dehydrodimer isomers presenting a dihydrobenzodioxane skeleton. The MS^{n} transitions for compounds 705-5 and 705-9 were 705→513→339→161 (Castillo-Fraire et al., 2019). These compounds are analogues of caffeic acid oxidation products already described by Cilliers and Singleton (1991).

In the following paragraph, all ^{1}H and ^{13}C chemical shifts are given for isomer 705-5. The corresponding chemical shifts for isomer 705-6 are listed in Table 1.

The ^{13}C NMR signal at 169.1 ppm was used as a starting point for the structure elucidation. It corresponded to a strongly deshielded carbon consistent with an ester group. Moreover, the ^{1}H-^{13}C HMBC spectrum showed a clear correlation of this carbon (169.1 ppm) with two adjacent protons presenting a large coupling constant ^{2}J (15.9 Hz) consistent with α-β ethylene protons. This carbon (169.1 ppm) was thus identified as C9 (Figure 3A) and the two protons at 7.6 ppm and 6.4 ppm were attributed to H7 and H8. HMBC correlations allowed H8 (6.4 ppm) to be unambiguously distinguished from H7 (7.6 ppm). Indeed, the latter was the only one showing HMBC correlations with two carbons (118.8 and 124.5 ppm) that were correlated to aromatic protons on the ^{1}H-^{13}C HSQC NMR spectrum assigned as H2 (7.26 ppm, d, 2 Hz) and H6 (7.2 ppm, dd, 8.5 and 2 Hz), respectively. The corresponding carbons C7 and C8 of protons H7 and H8 were at 146.8 ppm and 118.4 ppm, respectively. The ^{13}C signal at 130.9 ppm was attributed to the quaternary carbon C1.

Proton H2 (7.26 ppm, d, 2 Hz) was also correlated to ^{13}C signals at 145.6 ppm and 146.6 ppm that correspond to carbons C3 and C4, respectively. The ^{13}C NMR signal at 146.6 ppm was attributed to

carbon C4 as it was the only carbon showing an expected correlation with H6 (7.2 ppm). The ^{13}C signal at 145.6 ppm was thus attributed to C3.

The ^{1}H-^{13}C HMBC spectrum showed a correlation between carbon C6 (124.5 ppm) and another aromatic proton at 7.03 ppm that was assigned as H5 (d, 8.5Hz). This proton H5 was also correlated to two aromatic carbons assigned previously: C3 at 145.6 ppm and C4 at 146.6 ppm.

Conversely, the ^{13}C NMR signal at 169.5 ppm was used as a starting point for the structure elucidation of the other CQA moiety. It corresponded to a strongly deshielded carbon consistent with an ester group. The ^{1}H-^{13}C HMBC spectrum showed a clear correlation of this carbon (169.5 ppm) with three protons (4.9, 5.1, and 5.26 ppm). The proton at 5.26 ppm was assigned as H10', as this proton was correlated to the quinic acid part of the CQA moiety. The carbon at 169.5 ppm was thus assigned as C9'. The ^{1}H-^{13}C HMBC spectrum showed correlation of the proton at 5.1 ppm with six carbons (78.9, 116.4, 121.2, 128.7, 145.6, and 169.5 ppm). On the ^{1}H-^{13}C HSQC NMR spectrum, two of them (116.4 and 121.2 ppm) were correlated to aromatic protons at 6.79 ppm and 6.88 ppm, corresponding to H2' and H6'. The ^{13}C signal at 128.7 ppm was attributed to the quaternary carbon C1'. Based on these correlations, the two protons at 5.1 ppm and 4.9 ppm were attributed to H7' and H8', respectively. Their corresponding carbons C7' and C8' were assigned at 78.4 ppm and 78.8 ppm on the ^{1}H-^{13}C HSQC NMR spectrum.

Interestingly, a clear correlation was observed on the HMBC spectrum between H7' (5.1 ppm) and a carbon at 145.6 ppm that was previously assigned as C3. Additionally, a correlation between H8' (4.9 ppm) and a carbon at 146.6 ppm corresponding to C4 was observed. These two correlations constitute proof for the elucidation of the dihydrobenzodioxane structure (Figure 3B).

3.1.3 Structure elucidation of the dihydronaphtalene-type dehydrodimers

This pair of compounds presented UV–vis spectra with λmax around 318 nm and 342 nm (Castillo-Fraire et al., 2019). The complete NMR analysis of dehydrodicaffeoyldiquinic acid dimers 705-1 and 705-1.1 was used to confirm the structure of dehydrodimers showing a dihydronaphtalene nucleus (Figure 4A) based on the MS^n fragmentation, as discussed in a previous paper (Castillo-Fraire et al., 2019). The proposed structure was an analogue of caffeicin E resulting from caffeic acid oxidative coupling (Cilliers & Singleton, 1991). The MS^n transitions for 705-1 and 705-1.1 were 705→513→339→229 nm (Castillo-Fraire et al., 2019).

In the following part, the discussion concerns the ^1H and ^{13}C attributions for product 705-1. The same approach can be applied to product 705-1.1 that exhibited the same correlation scheme on the ^1H-^{13}C HMBC, ^1H-^{13}C HSQC, and ^1H-^1H COSY spectra. All details of chemical shifts and attribution of coupling constants are provided in Table 1.

Interestingly, in the present case, the ^1H NMR spectrum does not show any deshielded protons that would belong to a free α-β ethylenic system exhibiting a large coupling constant close to 16 Hz. This specific two-proton system was clearly observed and discussed before for products 705-3 and -4 and 705-5 and -6. This suggests that, in the case of 705-1, both ethylene linkages of the caffeoyl moieties have been modified in such a way that they are both involved in oxidative coupling.

This observation led us to select as a starting point the only strongly deshielded proton (singlet at 7.65 ppm) that also exhibited a clear HMBC correlation with a strongly deshielded carbon (169.2 ppm) consistent with an ester group. The proton was thus assigned as H7 and this deshielded carbon was attributed to C9. Then, carbon C9 clearly showed an HMBC correlation with another much more shielded proton at 3.95 ppm (doublet with J=3.4 Hz) that was attributed to H8'. Consequently, this coupling constant (3.4 Hz) allowed us to assign proton H7' at 7.47 ppm (doublet, J=3.4 Hz) and its corresponding carbon C7' located at 47.52 ppm using the ^1H-^{13}C HSQC spectrum. Noticeably, the ^1H-^{13}C HMBC spectrum showed that proton H7' was also correlated with nine carbons (Figure 4B).

Only one of them corresponded to a strongly deshielded carbon (174.8 ppm) that was thus attributed to C9'. Another weakly deshielded carbon (50.1 ppm) was attributed to C8', as its corresponding proton H8' was located at 3.94 ppm on the ^{1}H-^{13}C HSQC spectrum. The ^{13}C signals of the other seven carbons were located between 116 ppm and 136 ppm, consistent with aromatic or ethylene carbons.

Among them, C1', C8, and C6 could be distinguished from the others as they showed HMBC correlations with both H7' and H8'. C1' was easily distinguished as it presented typical correlations of an aromatic ABX system in a catechol group. C6 could be distinguished from C8 as only C6 exhibited HMBC correlations with three aromatic or ethylene protons, namely H5 (singlet 6.56 ppm), H2 (singlet, 6.88 ppm), and H7 (7.65 ppm). In contrast, C8 only showed correlation with one ethylene proton, namely H7 (7.65 ppm). H5 was distinguished from H2 as H5 showed HMBC correlation with C7'.

In contrast to the dihydrobenzofuran and the dihydrobenzodioxane structures, proton H8' in the dihydronaphtalene structure showed HMBC correlation with both C9 and C9' (ester group).

The complete NMR signal attributions of the protons and carbons belonging to the two catechol groups are not discussed here due to similarities with the structures of products 705-3 and -4, and 705-5 and -6 that have already discussed. All these attributions are given in Table 1.

3.1.4 Structure elucidation of the dehydrodimer presenting a symmetric structure

Although its molecular weight (MW 706 Da) and the presence of two quinic acid moieties were confirmed by mass spectrometry (Castillo-Fraire et al., 2019), compound 705-2 exhibited very different physicochemical features compared to the other CQA dehydrodimers. For instance, it was the only one showing a specific UV-Visible spectrum with a λmax at 282 nm and no more absorbance in the 300-340 nm region (Castillo-Fraire et al., 2019). This lack of absorbance at 320 nm for 705-2 indicated that the conjugated double bonds of the propenoic chains of the two CQA moieties were no

longer present in the dehydrodimer structure. Interestingly, this particular feature has already been observed for a dehydrodicaffeic acid oxidation product (Fulcrand et al., 1994).

In addition, the ^{1}H NMR spectrum was also original and differed from the other CQA dehydrodimers as it revealed a symmetric structure containing 24 non-hydroxyl protons. The ^{1}H and ^{13}C attributions and chemical shifts are given in Table 1. The complete 1D and 2D ^{1}H and ^{13}C NMR analyses allowed two hypothetical structures A and B to be proposed (Figure 5).

Except for some crucial NMR correlations, the following discussion mainly concerns the "non-prime" numbered moiety of the molecule. Considering the symmetry of the molecule, the argumentation is the same regarding the attribution of the "prime" numbered moiety.

The detailed structure of product 705-2 was elucidated from the ^{1}H and ^{13}C NMR spectra. The ^{1}H NMR spectrum revealed the presence of two aromatic protons at 6.77 ppm and one at 6.83 ppm. Their corresponding carbons were observed at 116.9, 117.3, and 121.9 ppm, respectively, on the ^{1}H-^{13}C HSQC NMR spectrum. HMBC correlations allowed C6 to be assigned at 116.9 ppm as this carbon was correlated with the two aromatic protons at 6.77 ppm (H2 and H5). The ^{1}H-^{13}C HMBC and ^{1}H-^{13}C HSQC NMR spectra permitted their corresponding carbons C2 and C5 to be assigned at 121.9 ppm and 117.3 ppm, respectively.

Carbon C6 (116.9 ppm) was also correlated with a deshielded proton at 6.27 ppm. The ^{1}H-^{13}C HMBC NMR spectrum showed that this proton has the particularity of being correlated with 7 carbons (55.3, 73.5, 116.9, 121.9, 131.4, 171.4, and 172.7 ppm). Among them, three corresponded to aromatic carbons that were attributed to C6 at 116.9 ppm, C2 at 121.9 ppm, and the quaternary carbon C1 at 131.4 ppm. The proton at 6.27 ppm was thus attributed to H7 (dd, 11 Hz and 1.7 Hz). The ^{1}H-^{13}C HSQC NMR spectrum allowed the chemical shift of its corresponding carbon C7 at 73.5 ppm to be determined.

Noticeably, proton H7 was correlated with two strongly deshielded carbons that have a ^{13}C NMR signal at 171.4 ppm and 172.7 ppm consistent with the carbon of ester groups. The ^{13}C signal at 171.4 ppm was attributed to C9 based on its clear HMBC correlation with proton H10 (4.72 ppm) of the quinic acid moiety through the oxygen atom. In contrast, the carbon at 172.7 ppm showed clear HMBC correlations with four shielded protons (at 1.75, 1.77, 2.53, and 2.57 ppm) attributed to the two CH2 groups (H11 and H13 protons) of the quinic acid moiety. This carbon at 172.7 ppm was attributed to C16 or C16' for hypothesis A or B, respectively.

In addition, proton H7 (6.27 ppm) was correlated to a moderately deshielded carbon at 55.3 ppm. The ^{1}H-^{13}C HSQC NMR spectrum permitted the chemical shift of its corresponding proton (3.89 ppm) to be determined. The ^{1}H-^{13}C HMBC NMR spectrum showed correlations between this proton (3.89 ppm) and four carbons (55.3, 73.5, 131.4, and 171.4 ppm). Among them, the NMR results highlighted the correlation with carbon C7 at 73.5 ppm, the quaternary carbon C1 at 131.4 ppm, and carbon C9 at 171.4 ppm. The proton at 3.89 ppm was thus attributed to H8. The H-H coupling constants of 11 Hz and 1.7 Hz measured for proton H8 (or H8') were the same as those measured for proton H7 (or H7') (Table 1). These coupling constants correspond to ^{2}J coupling (between H7 and H8 or H7' and H8') and ^{4}J coupling (between H7 and H8' or H8 and H7'). This can be considered as proof of the C8-C8'covalent bonding between both CQA moieties.

Another spot also confirmed the symmetric character of the molecule when the ^{1}H-^{13}C HMBC and HSQC NMR spectra were overlapped. Indeed, the ^{1}H-^{13}C HMBC spectrum revealed that the proton H8 (3.89 ppm) was correlated with a carbon presenting the same chemical shift at 55.3 ppm, proving that H8 was correlated with carbon C8' of the other CQA moiety.

Based on the NMR analysis, two "hypothetical" symmetric structures were proposed (Figure 5). Both structures showed two free catechol groups and both carboxylic groups of the quinic acid moieties are here included in two additional ester linkages. Neither the NMR analyses nor the MS^{n}

fragmentation pattern enabled one of the two proposed "hypothetical" symmetric structures to be discarded or favoured.

The hypotheses of both structures are based on the fact that the ^{1}H-^{13}C HMBC spectrum revealed a correlation between H7 and C16 or C16' and these two carbons cannot be distinguished due to the symmetry of the molecule.

A mechanism was proposed for these structures (Figure 5), starting with the PPO-catalysed oxidation of CQA leading to the formation of CQA ortho-quinone. This CQA ortho-quinone and another CQA molecule can generate two semiquinone radicals by a reverse disproportionation. Then, radical coupling can take place between carbons C8 and C8' of these semiquinones generating a covalent bond between these two molecules. Finally, a nucleophilic addition step occurs between the C16 (or C16') hydroxyl group and the C7 (or C7') position, followed by re-aromatization to yield the symmetric structure.

The particular presence of two catechol groups in this symmetric structure could confer tanning properties to this compound. Indeed, complexation between polyphenols and proteins is dominated mainly by hydrogen bonds and hydrophobic interactions involving the catechol groups of phenolic compounds (de Freitas & Mateus, 2012). These likely tanning properties could lead to specific interactions regarding salivary proteins and might have an impact on mouthfeel/sensations more or less related to astringency perception (Castillo-Fraire et al., 2021).

4 Conclusion

In a previous study, CQA dehydrodimers were synthesized in a biomimetic apple juice model solution (Castillo-Fraire et al., 2019). After purification and characterization using UV-Visible spectra and MS^{n} fragmentation, three hypothetical structures were proposed for nine of the ten dehydrodicaffeoyldiquinic acids (Castillo-Fraire et al., 2019).

In this study, we presented the structural confirmation of these hypotheses using 1D and 2D NMR spectroscopy. Four different structures were elucidated for dehydrodicaffeoyldiquinic acid compounds. Six of these CQA dehydrodimers corresponded to three different caffeicin-like skeletons: the dihydronaphtalene type for 705-1 and 705-1.1, the dihydrobenzofuran type for 705-3 and 705-4, and the dihydrobenzodioxane type for 705-5 and 705-6. Although our NMR data did not completely elucidate the stereochemistry of these molecules, the pairs of CQA oxidation products with the same skeleton are very likely stereoisomers resulting from the asymmetric C7' and C8' carbon centres. In addition, a phenolic structure corresponding to a symmetric dicatechol skeleton was highlighted for the first time as one of the dehydrodicaffeoyldiquinic acids resulting from CQA oxidative coupling.

Further studies are needed to better understand the relationships between structure and functional properties, regarding their contribution to organoleptic and nutritional qualities in apple-based beverages.

Funding sources

The authors wish to thank the Mexican Council for Science and Technology (CONACYT) (556831) for their financial support of a student via a graduate scholarship.

Acknowledgments

We are grateful to the P2M2 platform from the GIS Biogenouest (Le Rheu, France) for providing equipment and technical support for the chromatographic analyses.

Part of this work was performed using the PRISM core facility (Biogenouest©, UMS Biosit, Université de Rennes 1- Campus de Villejean- 35043 RENNES Cedex, FRANCE).

References

Bao, L., Li, J., Zha, D., Zhang, L., Gao, P., Yao, T., & Wu, X. (2018). Chlorogenic acid prevents diabetic nephropathy by inhibiting oxidative stress and inflammation through modulation of the Nrf2/HO-1 and NF-κB pathways. *International Immunopharmacology*, *54*(October 2017), 245–253. https://doi.org/10.1016/j.intimp.2017.11.021

Bernillon, S., Guyot, S., & Renard, C. M. G. C. (2004). Detection of phenolic oxidation products in cider apple juice by high-performance liquid chromatography electrospray ionisation ion trap mass spectrometry. *Rapid Communications in Mass Spectrometry*, *18*(9), 939–943. https://doi.org/10.1002/rcm.1430

Castillo-Fraire, C. M., Brandao, E., Poupard, P., Le Quére, J.-M., Salas, E., De Freitas, V., Guyot, S., & Soares, S. (2021). Interactions between polyphenol oxidation products and salivary proteins : Specific affinity of CQA dehydrodimers with cystatins and P-B peptide. *Food Chemistry*, *343*(128496), 1–11. https://doi.org/10.1016/j.foodchem.2020.128496

Castillo-Fraire, C. M., Poupard, P., Guilois-Dubois, S., Salas, E., & Guyot, S. (2019). Preparative fractionation of 5'-O-caffeoylquinic acid oxidation products using centrifugal partition chromatography and their investigation by mass spectrometry. *Journal of Chromatography A*, *1592*, 19–30. https://doi.org/10.1016/j.chroma.2019.01.071

Cilliers, J. J. L., & Singleton, V. L. (1991). Characterization of the Products of Nonenzymic Autoxidative Phenolic Reactions in a Caffeic Acid Model System. *Journal of Agricultural and Food Chemistry*, *39*(7), 1298–1303. https://doi.org/10.1021/jf00007a021

Clifford, M. N. (1999). Chlorogenic acids and other cinnamates–nature, occurrence and dietary burden. *Journal of the Science of Food and Agriculture*, *79*(3), 362–372. https://doi.org/10.1002/(SICI)1097-0010(19990301)79

Clifford, M. N. (2000). Chlorogenic acids and other cinnamates—nature, occurence, dietary burden, absorption and metabolism. *J Sci Food Agric.*, *80*(December 1999), 1033–1043.

de Freitas, V., & Mateus, N. (2012). Protein/Polyphenol Interactions: Past and Present Contributions. Mechanisms of Astringency Perception. *Current Organic Chemistry*, *16*(351), 724–746. https://doi.org/10.2174/138527212799958002

Fulcrand, H., Cheminat, A., Brouillard, R., & Cheynier, V. (1994). Characterization of compounds obtained by chemical oxidation of caffeic acid in acidic conditions. *Phytochemistry*, *35*(2), 499–505. https://doi.org/10.1016/S0031-9422(00)94790-3

Guyot, S., Bernillon, S., Poupard, P., & Renard, C. M. G. C. (2008). Multiplicity of Phenolic Oxidation Products in Apple Juices and Ciders, from Synthetic Medium to Commercial Products. In D. Fouad & L. Vincenzo (Eds.), *Recent Advances in Polyphenol Research* (pp. 278–292). Wiley-Blackwell. https://doi.org/10.1002/9781444302400.ch12

Le Bourvellec, C., Le Quéré, J. M., Sanoner, P., Drilleau, J. F., & Guyot, S. (2004). Inhibition of Apple Polyphenol Oxidase Activity by Procyanidins and Polyphenol Oxidation Products. *Journal of Agricultural and Food Chemistry*, *52*(1), 122–130. https://doi.org/10.1021/jf034461q

Naveed, M., Hejazi, V., Abbas, M., Kamboh, A. A., Khan, G. J., Shumzaid, M., Ahmad, F., Babazadeh, D., FangFang, X., Modarresi-Ghazani, F., WenHua, L., & XiaoHui, Z. (2018). Chlorogenic acid (CGA): A pharmacological review and call for further research. *Biomedicine and Pharmacotherapy*, *97*(August 2017), 67–74. https://doi.org/10.1016/j.biopha.2017.10.064

Pati, S., Losito, I., Palmisano, F., & Zambonin, P. G. (2006). Characterization of caffeic acid enzymatic oxidation by-products by liquid chromatography coupled to electrospray ionization tandem mass spectrometry. *Journal of Chromatography A*, *1102*(1–2), 184–192. https://doi.org/10.1016/j.chroma.2005.10.041

Poupard, P., Guyot, S., Bernillon, S., & Renard, C. M. G. C. (2008). Characterisation by liquid

chromatography coupled to electrospray ionisation ion trap mass spectrometry of phloroglucinol and 4-methylcatechol oxidation products to study the reactivity of epicatechin in an apple juice model system. *Journal of Chromatography A*, *1179*(2), 168–181. https://doi.org/10.1016/j.chroma.2007.11.083

Weber, F., Engelke, G. H., & Schieber, A. (2019). Structure elucidation and tentative formation pathway of a red colored enzymatic oxidation product of caffeic acid. *Food Chemistry*, *297*(124932). https://doi.org/10.1016/j.foodchem.2019.05.206

Wong-Paz, J. E., Muñiz-Márquez, D. B., Aguilar, C. N., Sotin, H., & Guyot, S. (2015). Enzymatic synthesis, purification and in vitro antioxidant capacity of polyphenolic oxidation products from apple juice. *LWT - Food Science and Technology*, *64*(2), 1091–1098. https://doi.org/10.1016/j.lwt.2015.07.007

Figure 1

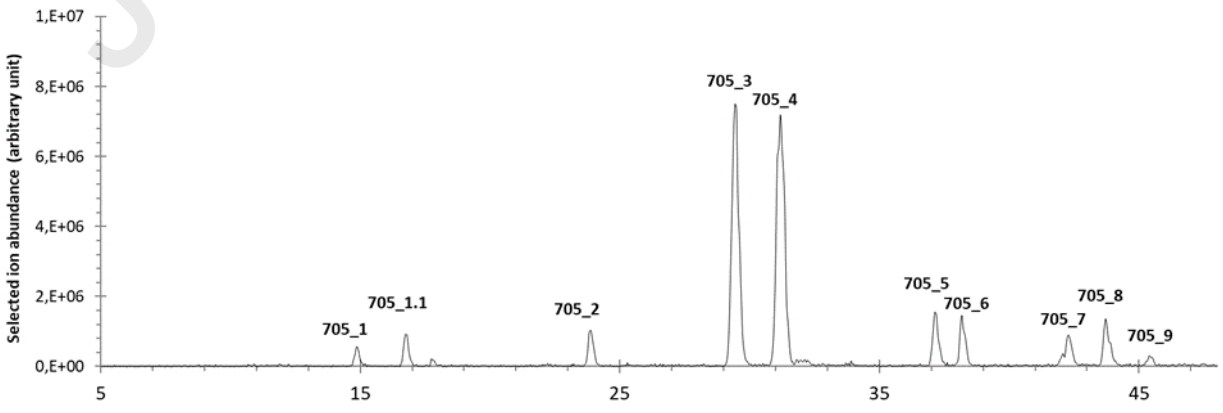

Figure 2

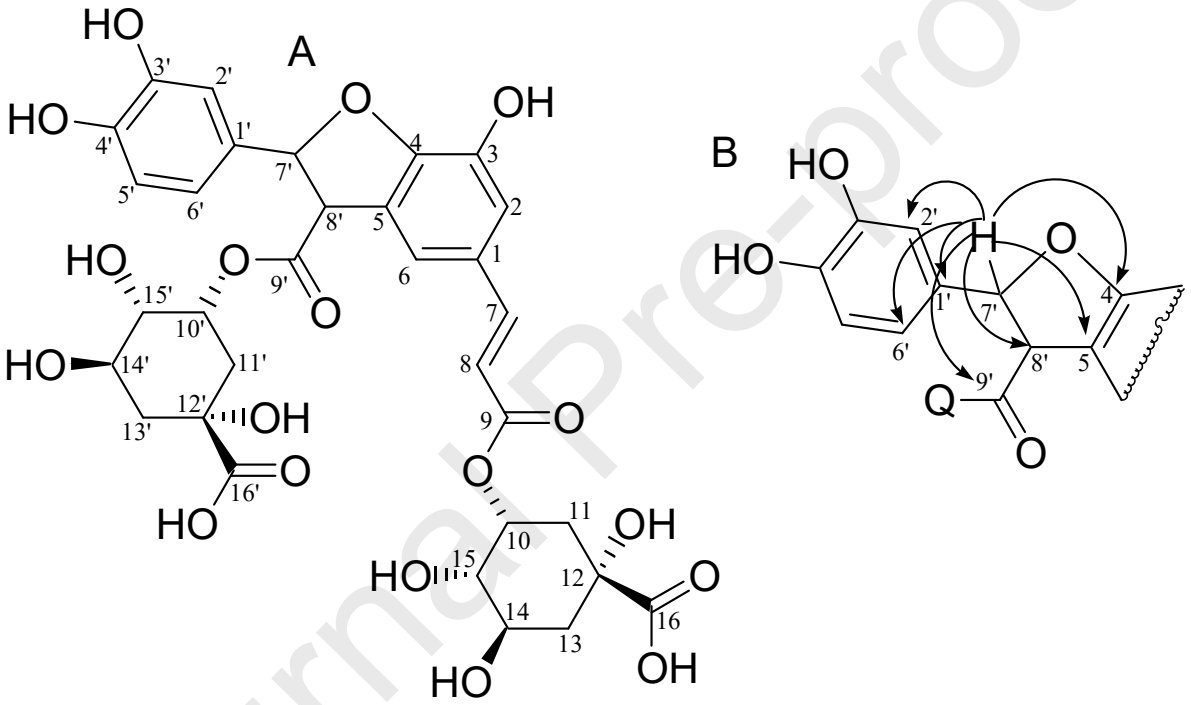

Figure 3

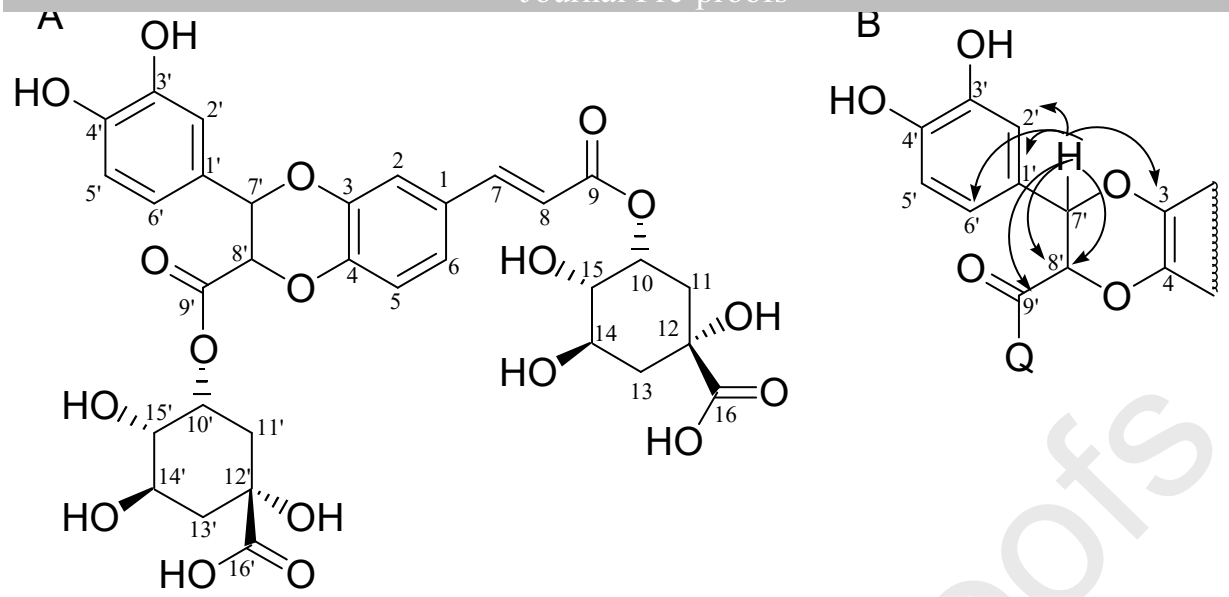

Figure 4

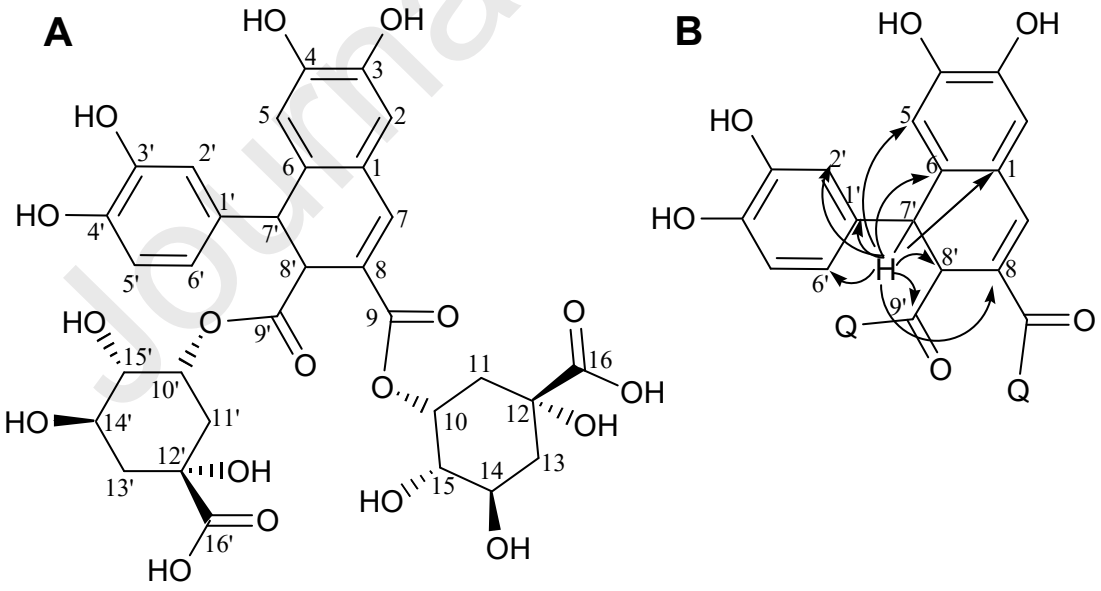

442 **Figure 5**

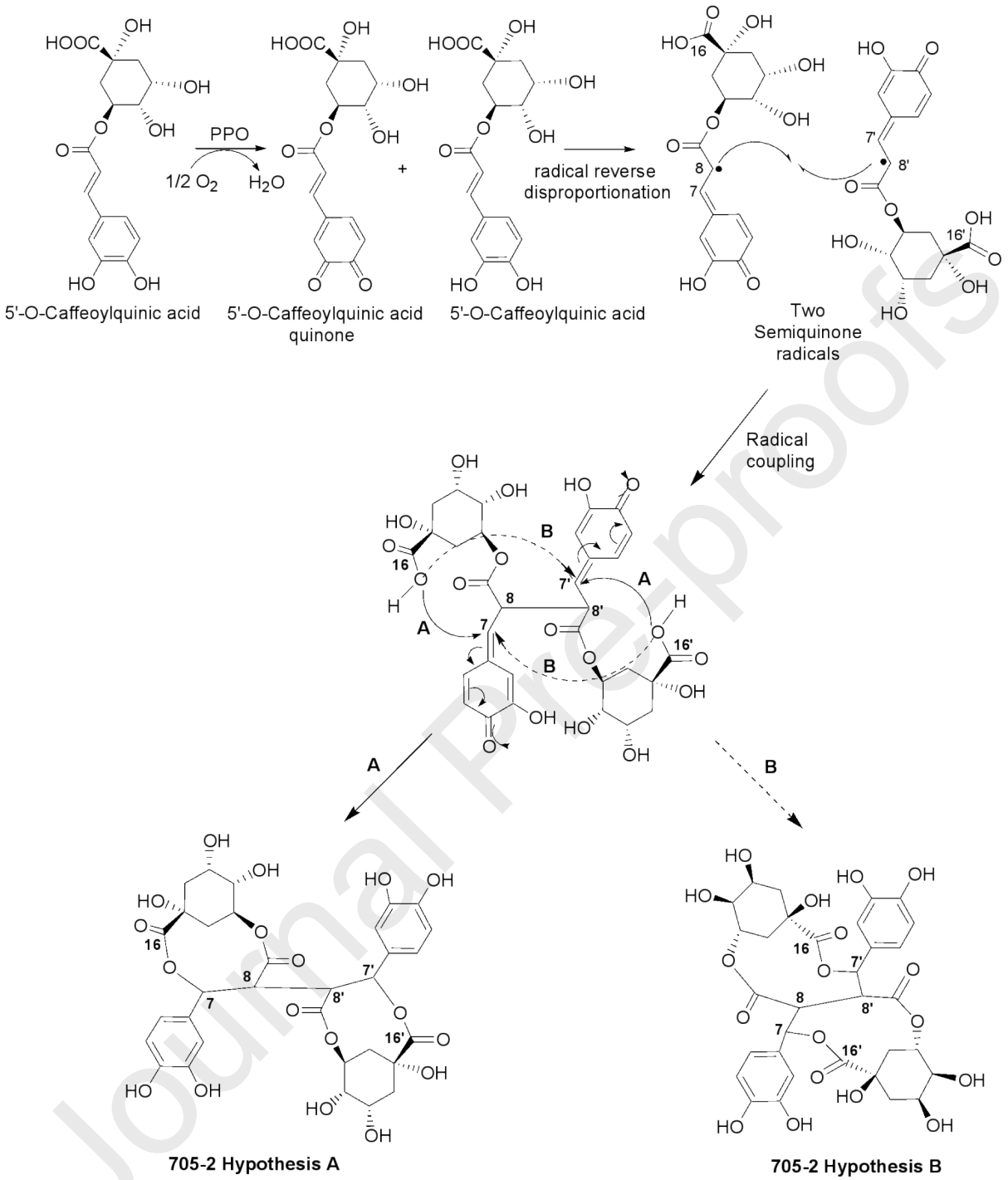

443

444

445 **Figures Captions**

446

447 **Figure 1.** Extracted ion MS chromatogram at m/z 705 ([M−H]⁻) from apple juice model solution
448 containing CQA oxidation products (706 Da).

449

450 **Figure 2. A**: Structure of products 705-3 and 705-4 corresponding to dehydrodicaffeoylquinic acids
451 showing a dihydrobenzofuran-type structure; **B**: HMBC correlations of proton H7' where **Q** is quinic
452 acid moiety.

453

454 **Figure 3. A**: Structure of products 705-5 and 705-6 corresponding to dehydrodicaffeoylquinic acids
455 showing a dihydrobenzodioxan-type structure; **B**: HMBC correlations of proton H7' where **Q** is a
456 quinic acid moiety.

457

458 **Figure 4. A**: Structure of products 705-1 and 705-1.1 corresponding to dehydrodicaffeoylquinic acids
459 showing a dihydronaphthalene-type structure; **B**: HMBC correlations of proton H7' where **Q** is a
460 quinic acid moiety.

461

462 **Figure 5.** Proposed mechanisms for the formation of two hypothetical structures corresponding to
463 product 705-2.

464

465

466 **Table 1.** Chemical shifts of protons (^{1}H) and carbon (^{13}C) for the seven CQA dehydrodimers
467 analysed.

Position	705-1				705-1.1				705-2				705-3				705-4			
	δC	δH	M	Hz	δC	δH	M	Hz	δC	δH	M	Hz	δC	δH	M	Hz	δC	δH	M	Hz
1	125,81	-	-	-	125,8	-	-	-	131,4	-	-	-	128,45	-	-	-	128,52	-	-	-
2	118,06	6,88	s	-	118,17	6,87	s	-	121,9	6,77	-	-	116,06	7,06	d	1,5	116,16	7,05	d	1,3
3	146,48	-	-	-	146,42	-	-	-	147,2	-	-	-	141,64	-	-	-	141,5	-	-	-
4	150,05	-	-	-	150,06	-	-	-	148,1	-	-	-	149,36	-	-	-	149,24	-	-	-
5	118,16	6,56	s	-	117,85	6,5	s	-	117,3	6,77	-	-	126,2	-	-	-	126,33	-	-	-

6	132,37	-	-	-	132,62	-	-	-	116,9	6,83	-	-	116,62	7,21	dd	1.2 ; 1.2	116,96	7,36	-	-
7	140,9	7,65	s	-	141,1	7,63	s	-	73,5	6,3	dd	11 ; 1.7	145,27	7,62	d	15,9	145,4	7,63	d	15,9
8	123,68	-	-	-	124,12	-	-	-	55,3	3,89	dd	11 ; 1.7	114,78	6,35	d	15,9	114,81	6,39	d	15,9
9	169,18	-	-	-	169,03	-	-	-	171,4	-	-	-	167,09	-	-	-	167,07	-	-	-
10	73,37	5,32	td	9.4 ; 4.3	73,51	5,32	td	9.0 ; 4.5	75,7	4,72	m	nd	70,68	5,37	dt	9.3 ; 4.5	70,72	5,37	dt	8.5 ; 4.5
11	39,89	2.27 ; 2.07	m	nd	39,62	2.22 ; 2.11	m	nd	31,6	2.53 ; 1.75	m	nd	37,44	2.26 ; 2.10	m	nd	37,15	2.23 ; 2.09	m	nd
12	77,18	-	-	-	77,14	-	-	-	74,5	-	-	-	74,81	-	-	-	74,56	-	-	-
13	39,08	2.19 ; 2.07	m	nd	39,05	2.20 ; 2.06	m	nd	39,3	2.57 ; 1.77	dt ; dt	14, 2.8 ; 14, 2.2	36,86	2.20 ; 2.07	m	nd	36,8	2.20 ; 2.07	m	nd
14	72,41	4,17	m	nd	72,27	4,18	m	nd	68,3	3,97	dt	12.2 ; 3.5	69,94	4,2	m	nd	69,55	4,18	-	-
15	74,41	3,75	dd	8.7 ; 3.1	74,2	3,79	dd	8.5 ; 3.2	69,4	3,39	-	-	72,1	3,77	dd	9.5 ; 3.2	71,704	3,76	-	-
16	178,07	-	-	-	177.96 or 178.07	-	-	-	172,7	-	-	-	175,77	-	-	-	175,66	-	-	-
1'	136,89	-	-	-	136,18	-	-	-	131,4	-	-	-	131,78	-	-	-	131,6	-	-	-
2'	116,82	6,48	d	2,1	117,16	6,53	d	2,1	121,9	6,77	-	-	112,58	6,86	d	1,5	112,54	6,86	-	1,5
3'	146,94	-	-	-	147,01	-	-	-	147,2	-	-	-	145,27	-	-	-	145,27	-	-	-
4'	145,91	-	-	-	146,1	-	-	-	148,1	-	-	-	145,45	-	-	-	145,48	-	-	-
5'	117,11	6,65	d	8,1	117,16	6,68	d	8,1	117,3	6,77	-	-	114,97	6,79	d	8,1	115	6,79	-	8,1
6'	121,03	6,45	dd	8.1 ; 2.1	121,47	6,49	dd	8.1 ; 2.1	116,9	6,83	-	-	117,34	6,79	dd	8.1 ; 1.5	117,31	6,79	-	8.1 ; 1.5
7'	47,52	4,47	d	3,4	48,26	4,38	d	5,6	73,5	6,3	dd	11 ; 1.7	86,96	6,05	d	7	87,17	6,04	d	7
8'	50,1	3,94	d	3,4	50,3	3,97	dd	5.5 ; 0.7	55,3	3,89	dd	11 ; 1.7	55,65	4,37	d	7	55,97	4,37	d	7
9'	174,8	-	-	-	175,43	-	-	-	171,4	-	-	-	170,57	-	-	-	170,5	-	-	-
10'	73,61	5,21	td	9.5 ; 4.5	73,65	5,17	td	9.4 ; 4.6	75,7	4,72	m	nd	71,92	5,43	dt	9.9 ; 4.9	72,07	5,39	dt	9.8 ; 4.7
11'	39,74	2.06 ; 1.96	m	nd	39,62	2.01 ; 1.83	m	nd	31,6	2.53 ; 1.75	m	nd	37,95	2.2 ; 2.1	m	nd	37,54	2.21 ; 2.06	m	nd
12'	77,15	-	-	-	77,18	-	-	-	74,5	-	-	-	75,08	-	-	-	74,82	-	-	-
13'	39,08	2.14 ; 2.03	m	nd	38,99	2.12 ; 2.03	m	nd	39,3	2.57 ; 1.77	dt ; dt	14, 2.8 ; 14, 2.2	36,86	2.2 ; 2.07	m	nd	36,8	2.17 ; 2.04	m	nd
14'	72,41	4,12	m	nd	72,41	4,1	m	nd	68,3	3,97	dt	11.7 ; 3.5	70,45	4,17	-	-	70,18	4,18	-	-
15'	74,41	3,62	dd	8.9 ; 3.2	74,43	3,63	dd	8.9 ; 3.2	69,4	3,39	-	-	72,46	3,79	dd	9.5 ; 3.2	72,07	3,76	-	-
16'	178,07	-	-	-	177.96 or 178.07	-	-	-	172,7	-	-	-	175,77	-	-	-	175,72	-	-	-

M: Multiplicity

Highlights

- Seven caffeoylquinic acid (CQA) dehydrodimers were analysed ^{1}H and ^{13}C NMR
- Four molecular skeletons of caffeoylquinic acid (CQA) dehydrodimers were elucidated
- Six compounds exhibited dihydrobenzofuran, benzodioxane or dihydronaphtalene nuclei
- A new CQA dehydrodimer showing a symmetric dicatechol skeleton was identified.
- Two structure hypotheses were formulated for this new molecule identified.

CRediT authorship contribution statement

Claudia Mariana Castillo-Fraire: Investigation, Methodology, Writing - original draft. Sandrine Pottier: Investigation, Writing - Review & Editing. Arnaud Bondon: Investigation, Writing - Review & Editing. Pascal Poupard: Supervision, Validation, Writing - review & editing. Erika Salas: Supervision, Writing - Review & Editing. Stéphane Bernillon: Investigation. Sylvain Guyot: Supervision, Conceptualization, Writing - review & editing.